The antiferromagnetic structure of $DyMn_2O_5$ at 4.2K

1981 J. Phys. C: Solid State Phys. 14 1671

(http://iopscience.iop.org/0022-3719/14/11/027)

J. Phys. C: Solid State Phys., **14** (1981) 1671–1683. Printed in Great Britain

The antiferromagnetic structure of $DyMn_2O_5$ at 4.2 K

C Wilkinson†, F Sinclair†‡, P Gardner†, J B Forsyth§ and B M R Wanklyn‖

† Queen Elizabeth College, London, W8 7AH, UK

§ Neutron Division, SRC Rutherford and Appleton Laboratories, Chilton, Didcot OX11 0QX, UK

‖ Clarendon Laboratory, Oxford, UK

Received 3 November 1980

Abstract. Powdered and single crystal specimens of dysprosium manganate, $DyMn_2O_5$, have been studied by neutron diffraction at temperatures between ambient and 4.2 K. Magnetic transitions are observed at 44 K, 18 K and 8.4 K. Both manganese and dysprosium moments are ordered below 8.4 K, where the magnetic structure has been refined. Measurements above 8.4 K indicate that this transition is to a second phase in which both moments are again ordered, but the details of the structure of this phase are not yet known. The relationship of the low-temperature phase to the magnetic structures of some isomorphous rare-earth manganates is discussed.

1. Introduction

Dysprosium manganate is a synthetic rare-earth transition metal oxide which crystallises in the orthorhombic system. Its crystal structure at 298 K has been refined by Abrahams and Bernstein (1967) using x-ray single-crystal methods. They find the cell dimensions to be $a = 7.2940 \pm 8$, $b = 8.551 \pm 8$, $c = 5.6875 \pm 8$ Å and table 1 gives the atomic positions within the space group Pbam. The atomic arrangement is illustrated in figure 1.

The magnetic properties of $DyMn_2O_5$ were first studied by Nowik *et al* (1966), who carried out bulk magnetisation and Mössbauer experiments on samples which they mistakenly described as $Dy_2Mn_4O_9$. They observed a large amount of magnetic anisotropy, the easy direction lying along ***a*** and the hard direction along ***c***; the temperature dependence of the magnetisation indicated an antiferromagnetic transition at 8 K. The Mössbauer absorption spectra for the ^{161}Dy nuclei exhibit paramagnetic relaxation behaviour at temperatures above 5 K and the authors point out that the magnetisation measurements do not show whether the Dy or the Mn atoms are responsible for the ordering transition at 8 K.

Bertaut *et al* (1965) claimed that in the isomorphous series RMn_2O_5, where R is a rare earth, the manganese atoms order antiferromagnetically below 46 K. Another isomorph, $BiMn_2O_5$, was indeed found to order by Bertaut *et al* (1967), but magnetic susceptibility measurements on the compounds with R = Sm, Tb, Ho and Lu by Schieber

‡ Present address: Department of Physics, Brandeis University, Waltham, Massachusetts, USA.

0022-3719/81/111671 + 13 $01.50

Table 1. The atomic positions in $DyMn_2O_5$, space group Pbam. The coordinates of the general position are: x, y, z; $-x, -y, -z$; $-x, -y, z$; $x, y, -z$; $\frac{1}{2}+x, \frac{1}{2}-y, -z$; $\frac{1}{2}-x, \frac{1}{2}+y, z$; $\frac{1}{2}-x, \frac{1}{2}+y, -z$; $\frac{1}{2}+x, \frac{1}{2}-y, z$.

Atom	Position	x	y	z
Dy	4g	0.13874	0.17169	0.0
Mn(I)	4f	0.0	0.5	0.2548
Mn(II)	4h	0.4119	0.3500	0.5
O(I)	4e	0.0	0.0	0.2741
O(II)	4g	0.1647	0.4452	0.0
O(III)	4h	0.1537	0.4354	0.5
O(IV)	8i	0.3951	0.2082	0.2414

et al (1973) failed to detect any magnetic transitions in the temperature range 1.4–300 K. However, direct evidence for the ordering of manganese moments was found by Buisson (1973), who reported a neutron diffraction study of powdered samples of the series of compounds with R = Nd, Tb, Ho, Er and Y. The extra peaks of magnetic intensity which were found in the low-temperature diffraction patterns could all be indexed in terms of incommensurate structures with propagation vectors $(\frac{1}{2}, 0, \tau)$. Table 2 gives the value of τ and the temperature at which it was measured for each of the compounds. Buisson obtained good agreement between the observed magnetic peak

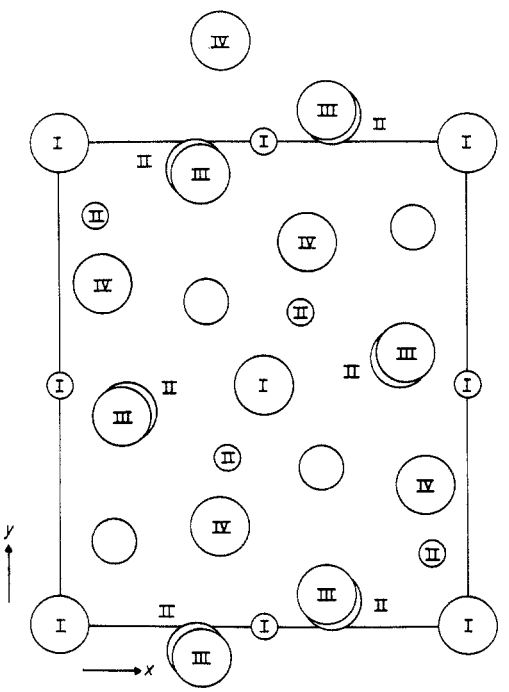

Figure 1. The [001] projection of the chemical structure of $DyMn_2O_5$ as determined by Abrahams and Bernstein (1967). The small circles represent manganese atoms, the large ones oxygen and the intermediate sized circles dysprosium. The Mn(I), O(I) and O(IV) atoms appear not only at the values of z given in table 1 but also exactly superposed with the value $\bar{z}$.

Table 2. Values of τ for the propagation vectors $[\frac{1}{2}\,0,\,\tau]$ found by Buisson (1973). The temperature at which τ was determined is also given.

Rare earth	τ	T (K)
Nd	0.365	21
Tb	0.306	18
Ho	0.271	1.5
Er	0.247	10
Y	0.32	4.2

intensities and those calculated for helical spin arrangements of moments on the manganese atoms, in which these moments rotate in the ***ab*** plane. Buisson (1973) also studied $LuMn_2O_5$ and found evidence for a more complicated antiferromagnetic structure which gives rise to magnetic peaks corresponding to propagation vectors $(\frac{1}{2}, 0, \tau)$ and $(\frac{1}{2}, 0, 0)$, but he did not determine this structure.

At 1.5 K the rare-earth moments in the Nd, Tb and Er manganates are also ordered without any change in the propagation vector τ (Buisson 1972). For $TbMn_2O_5$ and $ErMn_2O_5$, good agreement with the observed magnetic intensities could only be obtained with a model in which the rare-earth moment was amplitude modulated, whereas $NdMn_2O_5$ gave equally good agreement with either amplitude or spiral modulation of the Nd moments. His attempts to prepare pure samples of $DyMn_2O_5$ powder were unsuccessful, but he concluded that it is antiferromagnetic at 4.2 K and that the propagation vector is $(\frac{1}{2}, 0, 0)$.

The object of the present investigation has been to determine the low-temperature magnetic structure of $DyMn_2O_5$ using neutron diffraction techniques on both powdered and single-crystal samples. The material was prepared in single-crystal form from a $PbO—PbF_2—B_2O_3$ flux (Wanklyn 1972). The melt was first cooled to room temperature and then the crystals were hand-picked from other impurity phases, principally Mn_3O_4. The powdered material was obtained by crushing sufficient single crystals, thereby avoiding the impurity problem encountered by Buisson (1972).

2. Preliminary powder diffraction study

Thermal neutrons are highly absorbed by $DyMn_2O_5$, which has a linear absorption coefficient of 0.69 mm^{-1} at 1.18 Å. Diffraction data were therefore collected from a flat powder sample held in an aluminium container, of internal dimensions 2 × 25 × 50 mm height, and used in symmetrical transmission. The D2 diffractometer at the Institute Laue–Langevin, Grenoble, was used with an incident beam wavelength of 1.3 Å and the specimen was held in a variable-temperature helium cryostat. The powder pattern measured with a θ–2θ scan at 4.2 K is shown in figure 2. Several peaks which could not be indexed in terms of the room temperature nuclear structure were apparent; the peak intensities of two of the strongest of these ($2\theta = 16.4$ and 15.1°) were monitored as the temperature was raised and the variations of these intensities are shown in figure 3. Both curves show a sharp change in slope at 8.4 K but, whereas the intensity of the peak at $2\theta = 16.4°$ reaches a constant background level, there is a second but more gradual reduction in the intensity measured at $2\theta = 15.2°$ with the background level achieved only at 40 to 50 K. The complete powder patterns were then measured at 20 K and 60 K,

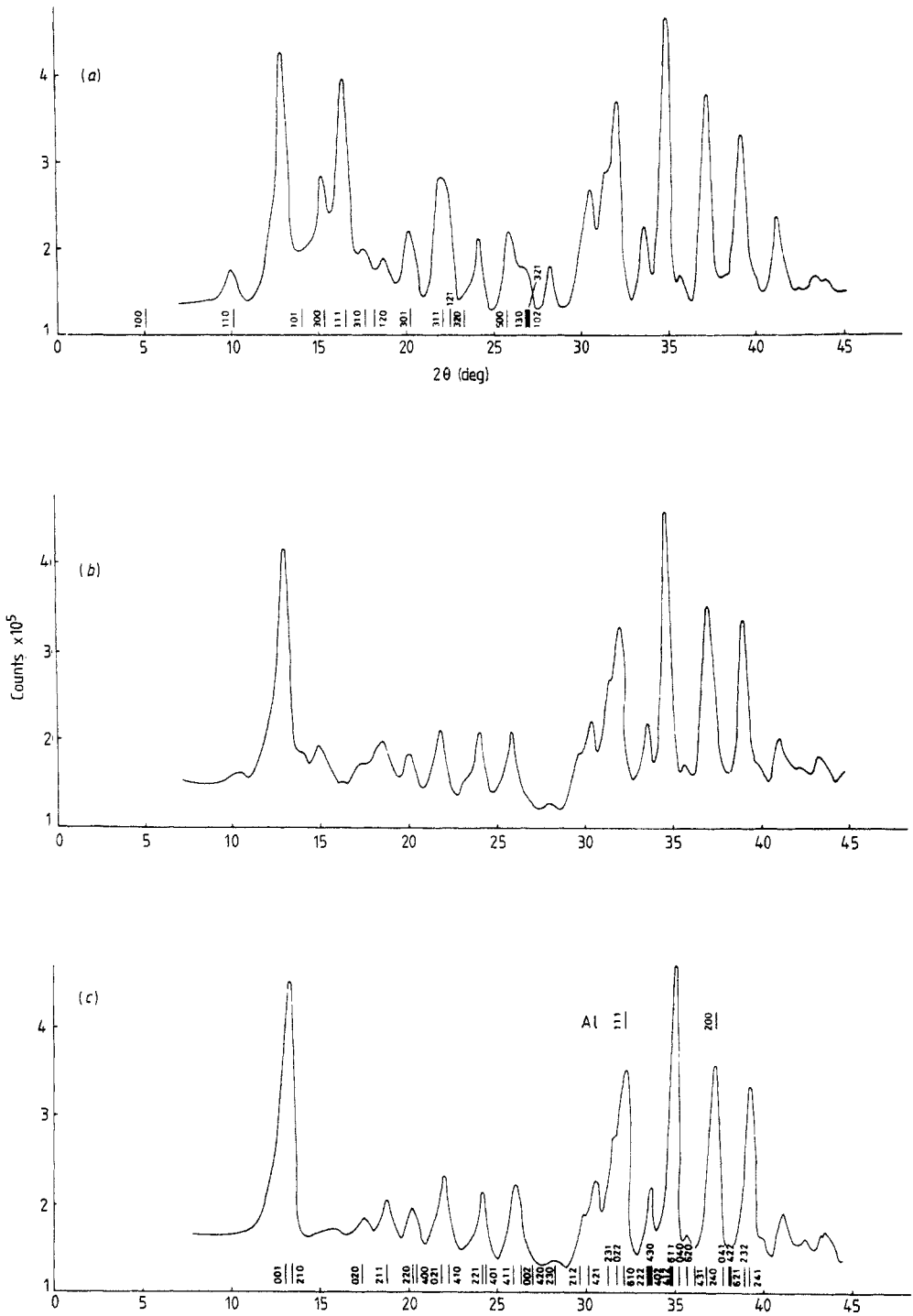

Figure 2. Neutron powder diffraction patterns from $DyMn_2O_5$ at (*a*) 4.2 K, (*b*) 20 K and (*c*) 60 K. The incident wavelength was 1.3 Å and the indexing corresponds to a magnetic unit cell with ***a*** twice that of the chemical cell.

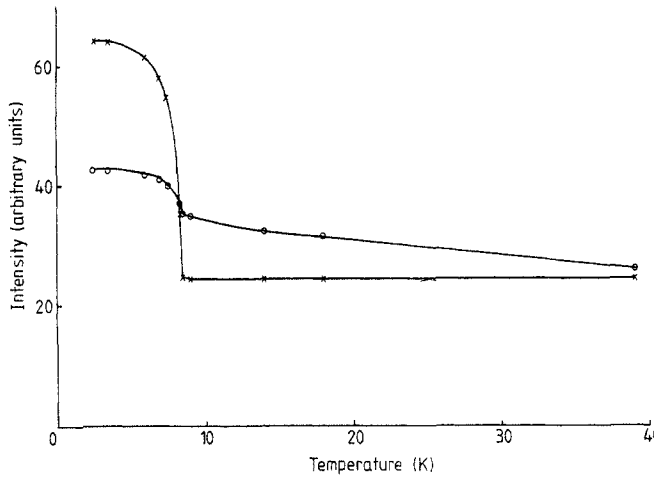

Figure 3. Temperature variation of the peak intensity at $2\theta = 15.2°$ (circles) and 16.4° (crosses) for the powdered sample of $DyMn_2O_5$. The scattering angles correspond to those for the (300) and (111) reflections respectively.

bracketing both the lower and upper apparent transition temperatures. These patterns are also shown in figure 2.

The chemical unit cell and atomic positions described by Abrahams and Bernstein (1967) enabled the pattern observed at 60 K to be indexed and good agreement to be obtained between observed and calculated intensities. The additional scattering at 4.2 K can be described in terms of a magnetic cell with an '*a*' axial length twice that of the chemical cell, corresponding to a spiral with propagation vector $\tau = (\frac{1}{2}, 0, 0)$. The indexing scheme shown in figure 2 corresponds to this cell. By a comparison of the total nuclear and magnetic intensities, it can be estimated that the magnetic scattering power of one formula unit of $DyMn_2O_5$ is at least 90 μ_B^2. This value indicates that the dysprosium atom moments are ordered, since it is too large to be accounted for by manganese moments alone.

The additional scattering in the 20 K pattern is much less than that at 4.2 K ($\sim$ 20 μ_B^2 per formula unit) indicating that the disprosium moments are not ordered at this temperature. Peaks at $2\theta = 10.5$, 14 and 15° are visible, but could not be indexed in terms of a spiral structure with $\tau = (\frac{1}{2}, 0, 0)$.

3. Single-crystal measurements

3.1. Integrated intensities

Dysprosium manganate crystals have a prismatic habit, bounded by {110} {120} {100} and {010} faces and terminated by {001}. A crystal with overall dimensions 2.3 × 1.9 × 3.3 mm in the ***a***, ***b*** and ***c*** directions respectively was selected and mounted with [001] as rotation axis in a variable-temperature helium cryostat on the D15 diffractometer at ILL. Integrated intensity data were collected at 4.2 K, 15 K, 60 K and at room temperature and were first corrected for absorption, since even the small size of crystal used gave transmission factors which varied between 0.39 and 0.32. A comparison of

the observed intensities for a set of nuclear reflections at room temperature with those calculated from the Abrahams and Bernstein (1967) structure showed that a significant extinction correction was needed. However, an empirical curve relating I_{obs} and I_{cal} could be plotted from the nuclear data and subsequently used to correct the observed magnetic intensities since, in all but two instances, these lay in the same intensity range.

3.2. Variation of the magnetic structure with temperature

A study was also made of the evolution of the intensities of selected magnetic reflections as a function of temperature. As indicated in the powder pattern, below 8.4 K the major part of the magnetic scattering was found to be contained in satellite reflections corresponding to a spiral with propagation vector $(\frac{1}{2}, 0, 0)$. The single-crystal study revealed additional, though much weaker, satellites in this temperature range at positions corresponding to a spiral propagation vector $(\frac{1}{2}, 0, \tau)$, with the value of $\tau = 0.250 \pm 0.002$. At these temperatures the scattering therefore resembles that observed by Buisson in the case of $LuMn_2O_5$.

The crystal was re-mounted about an [010] axis and the integrated intensities of the $(h/2, 0, l \pm \tau)$ satellite reflections were measured at 4.2 K. A high resolution scan of the distribution of intensity associated with positions $(h/2, 0, l \pm \tau)$ showed that there are in fact closely spaced pairs of satellite reflections at $((h \pm \delta)/2, 0, l \pm \tau)$ with $\delta \sim 0.001$, which change their positions and relative intensities in a complex way as the temperature is raised.

At 8.4 K the magnetic scattering in the $(h/2, k, 0)$ positions disappears, while the intensity in positions $((h \pm \delta)/2, 0, l \pm \tau)$ persists, but changes in magnitude. A second set of measurements of the integrated intensity around positions $(h/2, 0, l \pm \tau)$ was made at 15 K.

On further raising the temperature, a second magnetic phase change appears to take place at 18.0 ± 0.5 K when the $\pm\delta/2$ satellites amalgamate to give single diffraction peaks. The intensities of these peaks then fall steadily and finally disappear at 44 ± 2 K.

4. The magnetic structure at 4.2 K

The comparison of the nuclear reflections at 4.2 K with those measured at room temperature and 60 K showed that there was no additional intensity in the nuclear reflection positions at the lowest temperature.

The magnetic intensities at 4.2 K which had been corrected for absorption and extinction were placed on an absolute scale by comparison with the nuclear peaks. The observed squares of the magnetic structure factors, F_M, for the $\{h/2, k, 0\}$ and $\{h/2, 0, l \pm \tau\}$ reflections were used to calculate two-dimensional spin density Patterson functions (Wilkinson 1968, 1973) as shown in figures 4(*a*) and (*b*). These two functions relate to spin structures which to a first approximation make orthogonal contributions to the scattered intensity and can therefore be analysed independently.

4.1. Patterson generated from {h/2, k, 0} reflections

These reflections account for some 85% of the total magnetic intensity. It is evident from figure 4(*a*) that, excluding the origin peak, there are four strong peaks, A, B, C and D

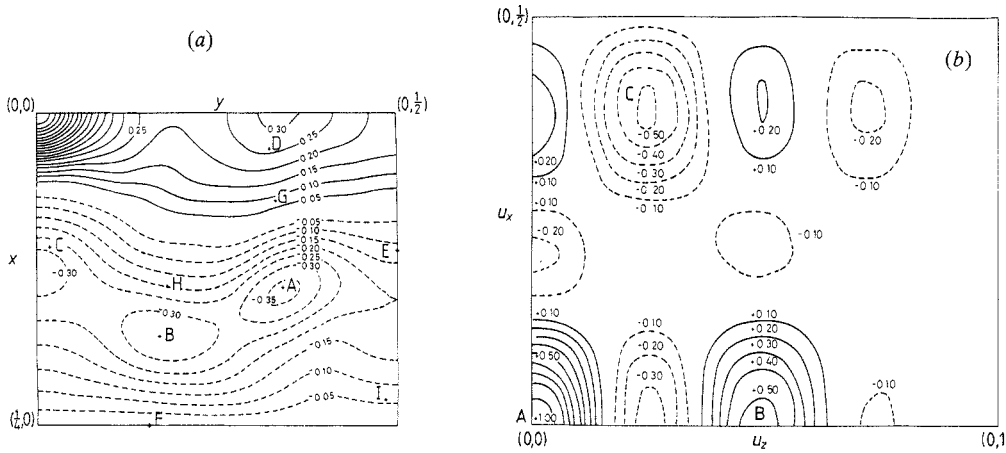

Figure 4. (*a*) [100] projection of the spin density Patterson function for $DyMn_2O_5$ at 4.2 K. The principle interatomic vectors Dy–Dy and Dy–Mn are indicated and the contours are expressed as fractions of the origin height. (*b*) [010] projection of the spin density Patterson function for $DyMn_2O_5$ at 4.2 K calculated from $\{h/2, 0, l \pm \tau\}$ reflections. All interatomic vectors are indicated by crosses. Contours are expressed as fractions of the origin height.

in the spin density Patterson map. Wilkinson (1968) has shown that the peak height due to two spins $\boldsymbol{S}^0$ and $\boldsymbol{S}'$ is proportional to

$$H = \tfrac{1}{2}(S_x^0 S_x' + S_y^0 S_y') + S_z^0 S_z' \tag{1}$$

Considering only interatomic vectors that have a dysprosium atom as an endpoint, it is easy to identify these peaks with interatomic vectors from the origin (table 3).

One of the peaks is positive, indicating magnetic moments separated by an appropriate vector with a positive scalar product, and three of them negative. The peak heights are expressed as a fraction of the height of the origin peak, which is always the largest as it is proportional to the sum of all the input intensities. The coordinates are referred to the magnetic unit cell which was used throughout the calculation. The absence of magnetic intensity in the h integral (nuclear) reflections indicates an antiferromagnetic coupling along the x direction which constrains the spins in one half of the magnetic cell to be exactly the inverse of those in the other half. This alternation with a periodicity of $2\boldsymbol{a}$ (chemical) does not, however, place any restriction on the twelve spins of the chemical cell. A non-linear least-squares refinement was carried out, using at first all the constraints derivable from the spin density Patterson. The interatomic vector that showed a positive coupling produced a constraint that held the pairs of spins parallel, while those

Table 3.

Peak label	Atoms	x	y	z	Peak amplitude	Multiplicity
A	Dy–Dy	0.14	0.34	0.0	−0.36	2
B	Dy–Mn_I	0.18	0.17	±0.25	−0.34	8
C	Dy–Mn_{II}	0.11	0.02	0.5	−0.30	4
D	Dy–Mn_{II}	0.03	0.32	0.5	+0.27	4

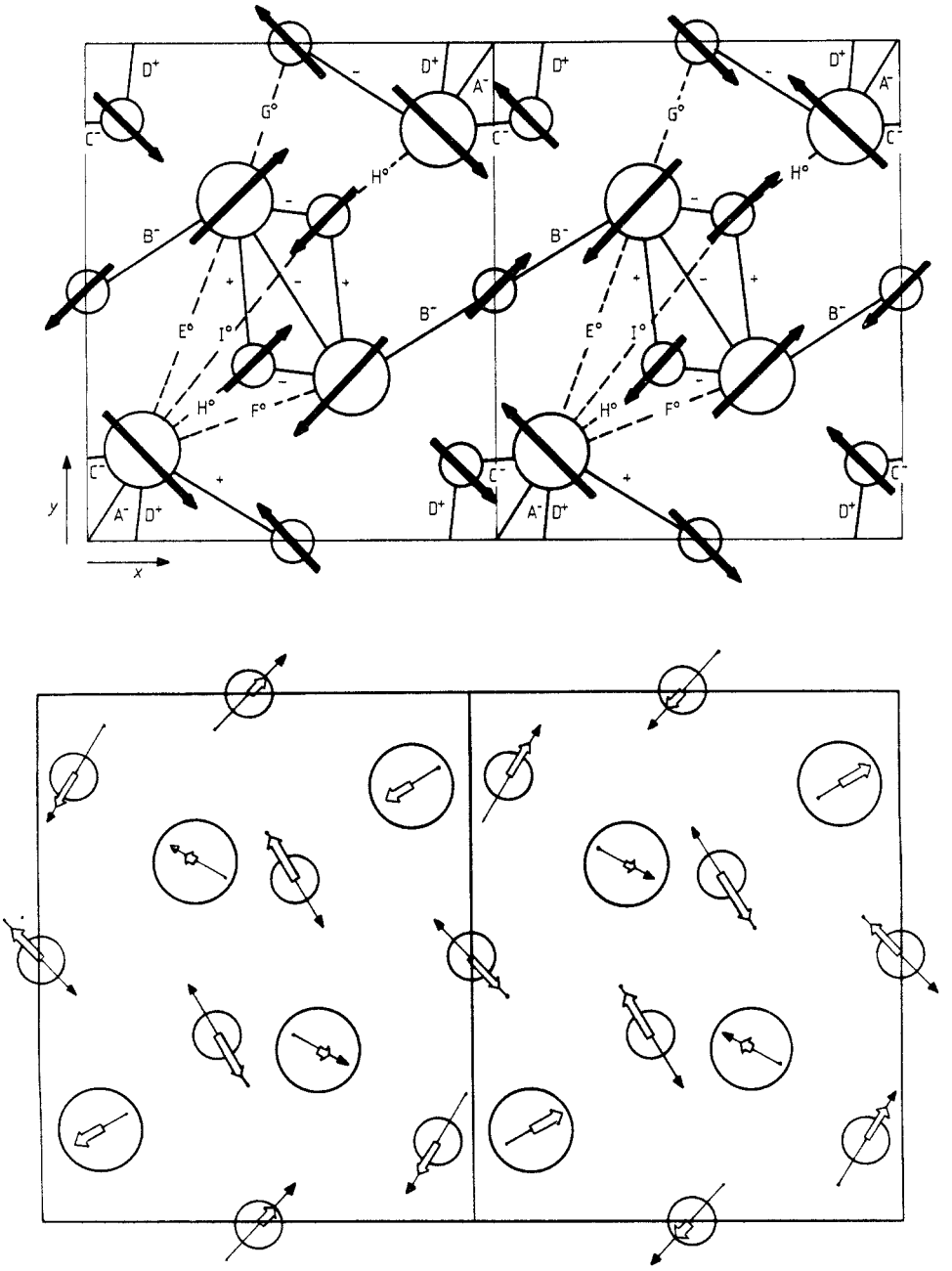

Figure 5. (*a*) Interatomic vectors involving at least one dysprosium atom. The $^-$, $^-$ and $^\circ$ superscripts to the vectors indicate ferromagnetic, antiferromagnetic or 90° coupling respectively between the moments and were derived from the Patterson function shown in figure 4(*a*). The trial magnetic structure is also shown. (*b*) The component of the magnetic structure refined from the $\{h/2, 0, l \pm \tau\}$ magnetic reflections. There is an arbitrary phase angle of coupling between this structure and that shown in 5(*a*). The maximum amplitude of the moment at each site is proportional to the length of the arrowed line, which also indicates the positive direction. The open arrows represent a snapshot of the moments in two unit cells when the phase origin is defined by $\gamma_1 = 0.0$.

Table 4.

Peak	Atoms	x	y	z	Multiplicity
E	Dy–Dy	0.11	0.50	0.0	4
F	Dy–Dy	0.25	0.16	0.0	4
G	Dy–Mn_I	0.07	0.33	±0.25	8
H	Dy–Mn_{II}	0.14	0.18	0.50	4
I	Dy–Mn_{II}	0.23	0.48	0.50	4

showing a negative peak height were interpreted as constraints holding the appropriate spins antiparallel. All the interatomic vectors involving Dy are identified in figure 5(a), which also shows the sign of the associated peak. No peaks are observed corresponding to five interatomic vectors involving dysprosium (table 4). The spins on these atom pairs were therefore constrained by relations of the sort

$$\tfrac{1}{2}(S_x^0 S_x' + S_y^0 S_y') + S_z^0 S_z' = 0 \tag{2}$$

so that they were held at approximately right angles.

The trial magnetic configuration derived from these considerations is also shown in figure 5(a). The constraints reduced the number of independent parameters from 36 to 12, and after several cycles of refinement an R factor on intensities of 0.08 was reached. Constraints of the sort described by equation (2) served only to ensure that the refinement process did not stray too far from the values of the parameters that produce a Patterson function similar to that observed. When these latter constraints were removed, increasing the number of independent parameters to 18, some small reorientations of the spins took place, but in neither refinement did the S_z spin components take on large values. Furthermore, the S_x and S_y components for the atom pairs which were not constrained to have parallel or antiparallel spins suggested that the ***b*** glide perpendicular to ***a*** in the chemical space group is retained in the magnetic symmetry; the double ***a*** repeat means that the ***b*** glide is alternately b and b'. Introducing this symmetry relationship and setting all the S_z components to zero reduces the number of parameters to six yet the final R factor increased only slightly from 0.080 to 0.084, confirming that the twelve parameters which had been removed were indeed unnecessary.

The dysprosium and Mn_{II} atoms lie in the mirror plane of the chemical space group. Their moments are found by experiment to lie in this plane, which is therefore likely to be an antioperator, m', in the magnetic group. The pairs of Mn_I atoms which are overlapped in the [001] projection are related to each other by this mirror plane which would require that their S_x and S_y components be equal and that any S_z components be equal but opposite in direction. The individual spin components of the Mn_I atoms can be determined from the additional $\{hk1\}$ reflection data. The individual spin moments of these Mn_I pairs were displaced in opposite directions in the (001) plane about the mean values obtained from the $\{hk0\}$ refinement and the refinement enlarged to include the $\{hk1\}$ data. The moments of the Mn_I pairs returned to parallelism irrespective of the starting values, consistent with the existence of m' in the magnetic space group. The possibility of finite S_z components on the Mn_I atoms was also explored, but resulted in no significant improvement in the R factor.

The final R factor for all 80 independent magnetic reflections was 0.084 when the intensities were weighted by their estimated variances. The calculated and observed

Table 5(*a*). The major components of moment on each magnetic atom in the magnetic structure of $DyMn_2O_5$ at 4.2 K as deduced from $\{h/2\ k\ 0\}$ reflections.

Atom type	Coordinates			Moment components (μ_B)	
	x	y	z	μ_x	μ_y
Dy	0.1387	0.1717	0.0000	4.51(3)	−8.02(1)
	0.8613	0.8283	0.0000	4.51	−8.02
	0.6387	0.3283	0.0000	−4.51	−8.02
	0.3613	0.6717	0.0000	4.51	8.02
Mn_I	0.0000	0.5000	0.2548	−1.44(4)	−1.35(1)
	0.0000	0.5000	0.7452	−1.44	−1.35
	0.5000	0.0000	0.2548	−1.44	1.35
	0.5000	0.0000	0.7452	−1.44	1.35
Mn_{II}	0.0881	0.8500	0.5000	2.10(4)	−1.26(1)
	0.4119	0.3500	0.5000	2.10	1.26
	0.5881	0.6500	0.5000	−2.10	−1.26
	0.9119	0.1500	0.5000	2.10	−1.26

Table 5(*b*). The amplitude modulated components (oriented at right angles to the components given in 5(*a*)) as deduced from the $\{h/2, 0, l \pm \tau\}$ reflections. The phase of the Mn_I atom at (1/2, 0, 0.7452) has been arbitrarily set to zero.

Atom type	Amplitude modulated components (μ_B)		Phase angle γ (deg)
	μ_x	μ_y	
Dy	−1.4(1)	−0.8(1)	10
	−1.4	−0.8	10
	−1.4	+0.8	73
	+1.4	−0.8	73
Mn_I	−1.8(1)	+1.9(1)	114
	−1.8	+1.9	70
	+1.8	+1.9	44
	+1.8	+1.9	0
Mn_{II}	−1.4(1)	−2.3(1)	3
	+1.4	−2.3	102
	−1.4	+2.3	102
	−1.4	−2.3	3

values for the two strongest magnetic intensities, which were not included in the refinements, lay close to an extrapolation of the empirical curve relating the calculated and observed nuclear intensities.

The magnetic structure is essentially as illustrated in figure 5(*a*) and table 5(*a*) gives the component of moment on each magnetic atom. The errors on the components have been estimated in the least-squares fitting program and the magnitudes of the spins and their errors are:

Dy 9.20(2) μ_B
Mn_I 1.97(4) μ_B
Mn_{II} 2.45(4) μ_B

4.2. Patterson generated from $\{h/2, 0, l \pm \tau\}$ reflections

These reflections contribute some 15% to the total magnetic intensity. The positions of Patterson vectors are again shown as crosses in figure 4(*b*). Selecting the three most prominent features (including the origin), labelled A, B and C on the diagram, allows approximate equations relating the magnitudes of the moments on the Dy and Mn_I and Mn_{II} atoms to be established.

Assuming that the components of the moments on atoms related by the chemical centre of symmetry are coupled in the same way as those described in § 4.1, the equations are

$$Mn_I^2 + Mn_{II}^2 + Dy^2 \simeq 1.00 \qquad \text{(A)}$$

$$(Mn_I^2 + DyMn_{II} \cos 30°) \cos 45° \simeq 0.53 \qquad \text{(B)}$$

$$(Mn_IMn_{II} + DyMn_I) \cos 22.5° \simeq 0.43 \qquad \text{(C)}.$$

The equations have solution Dy ~ 0.35, Mn_I ~ 0.71 and Mn_{II} ~ 0.49. Several possibilities were tried, but the best fit to the observed intensities was obtained by inserting these relative values in a model in which the moment $\boldsymbol{\mu}_j$ of the jth atom is described by an amplitude modulated function

$$\boldsymbol{\mu}_j = \mu_j \hat{\boldsymbol{m}}_j \cos(2\pi\boldsymbol{\tau} + \boldsymbol{r}j + \gamma j)$$

where $\hat{\boldsymbol{m}}_j$ is a unit vector at right angles to the moment component on the jth atom described in § 4.1, τ is the propagation vector of the spiral, $\boldsymbol{r}_j$ is the position of the atom in the unit cell and γ_j is its phase angle. It was immediately apparent from the calculation of structure factors using this model that $\hat{\boldsymbol{m}}_j$ had to lie in the ***ab*** plane to produce agreement with the observed data. A least-squares fit with eight parameters produced an R factor of 0.15 for 20 independent reflections. This agreement matched the fractional variation in the measured equivalence of these weak reflections. The parameters of the fit are shown in table 5(*b*) and a diagram showing the spin configuration is given in figure 5(*b*).

5. Discussion

The magnetic structure of dysprosium manganate at 4.2 K has been well established despite the relatively large corrections which had to be made for extinction. The magnetic space group is $P_{2a}b'2_1m'$ which is illustrated in the conventional orientation, $P_{2b}m'c'2_1$, in figure 6. The structure as refined bears little superficial resemblance to those proposed by Buisson (identified as B in the following text) for the series of isomorphous compounds RMn_2O_5 (R = Nd, Tb, Ho, Er, Y), but seems to be more closely related to that of $LuMn_2O_5$. However, consideration of the local coupling within the magnetic cell of $DyMn_2O_5$ shows that it has many features in common with the structures B. Both the commensurate and incommensurate structures have their magnetic moments in the ***ab*** plane and have these moments inverted on translation by ***a*** (chemical). In the structures B, Mn_I (Mn^{4+}) atom pairs displaced by ± 0.25 in z from the plane of the rare-earth atoms have their moments separated by an angle lying in the range 7.5° (Nd) to 42° (Ho) when the rare-earth moments are not ordered. This predominantly ferromagnetic coupling is enhanced below the rare-earth ordering temperature in Tb and Er manganates (Buisson 1972) and the angle between the spins decreases; in $DyMn_2O_5$ the spins are parallel.

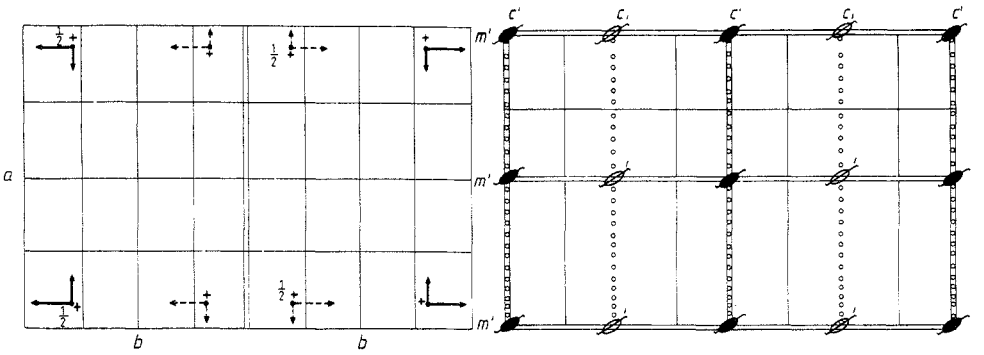

Figure 6. The magnetic space group of $DyMn_2O_5$, $P_{2b}m'c'2_1$. The symbols are those used by Atoji (1965).

Figure 7 shows the $Mn_{II}(Mn^{3+})$ spin directions when only manganese ions participate in the magnetic structures B. Buisson (1973) found values for the angle φ which range from 23° (Tb, Er) to 0° in YMn_2O_5, where the spins are in the same relative orientation as in $DyMn_2O_5$.

Our observation of a transition at 44 K suggests that the ordering of the Dy moments at 8.4 K is also preceded by an ordering involving only Mn atoms, as Buisson finds for the Nd, Tb and Er compounds. A preliminary analysis of the $(h/2, 0, l \pm \tau)$ satellite data collected at 15 K, however, suggests that good agreement can be obtained only when there is a small dysprosium moment in addition to those on the Mn_I and Mn_{II} atoms. It seems possible, therefore, that the phase change which is observed at 18 K could be connected with the appearance of a small induced moment on the dysprosium atoms.

The overall maximum moment values of Dy and Mn atoms are obtained by combining the components described in figures 5(*a*) and 5(*b*). These are as follows: Dy, $9.32(2)\mu_B$; Mn_I, $3.26(11)\mu_B$; Mn_{II}, $3.64(11)\mu_B$.

The observed magnetic moment associated with the Dy atoms is in good agreement with a value of $J = 15/2$ corresponding to the Dy^{3+} ion. At $T/T_c = 0.5$ we would expect

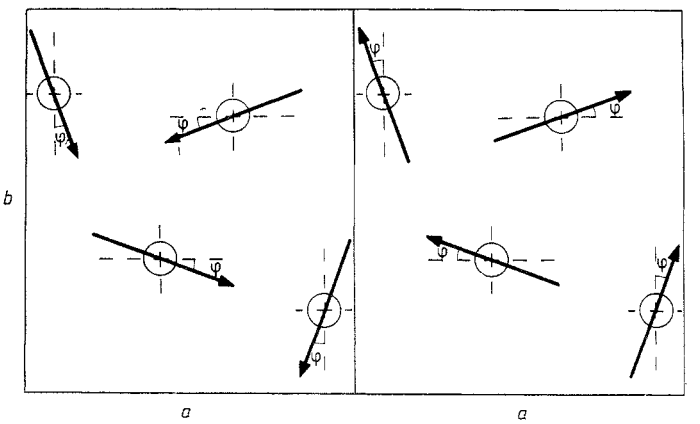

Figure 7. The magnetic coupling between Mn_{II} atoms in the incommensurate structures found by Buisson (1973). The angle φ ranges from 23° in $TbMn_2O_5$ and $ErMn_2O_5$ to 0° in YMn_2O_5.

that the observed moment would be some 0.83 of the saturation value, i.e. 8.82 μ_B, compared with the observed value of 9.32 μ_B. This is of course a maximum value, since there is a small amount of amplitude modulation present, although this is not as large as the amplitude modulation of the rare-earth moments deduced by Buisson (1972) on the basis of his powder data for the Tb and Er compounds. It is hoped to augment the latter studies by single-crystal measurements and suitable samples have already been prepared.

The observed moments of Mn_I (3.26(11) μ_B) and Mn_{II} (3.64(12) μ_B) are in quite good agreement with the Mn^{4+} and Mn^{3+} spin-only moments of 3 μ_B and 4 μ_B respectively. The corresponding ranges of values in the B structures are 1.9–2.8 μ_B and 2.5–3.4 μ_B respectively, though μMn^{3+} is always greater than μMn^{4+} in any given structure. Of course, the moments deduced for the Mn^{4+} and Mn^{3+} ions depend on the atomic form factor used in the fitting procedure. A single Mn^{3+} 3d form factor (Watson and Freeman 1961) has been used in this work. An approximate Mn^{4+} 3d form factor decreases our values for the Mn moments by some 0.1 μ_B, but does not improve the agreement between the observations and the model. The total observed moment, per $DyMn_2O_5$, of 16.2 μ_B is double the saturation moment of 8 μ_B for a field of 10 T applied parallel to ***a*** found by Nowik *et al* (1966). Although ***a*** is the easy direction of magnetisation, it is therefore clear that 10 T is not sufficient to produce complete spin alignment at 4.2 T.

Acknowledgments

The authors wish to thank the Institut Laue–Langevin, Grenoble, for the provision of research facilities. One of us (PG) is also indebted to the Institut for financial support as a Collaborateur de Thèse.

References

Abrahams S C and Bernstein J L 1967 *J. Chem. Phys.* **46** 3776
Atoji M 1965 *Am. J. Phys.* **33** 212
Bertaut E F, Buisson G, Durif A, Mareshal J, Montmory M C and Quezel-Ambrunaz S 1965 *Bull. Soc. Chim. Fr.* 1132
Bertaut E F, Buisson G, Quezel-Ambrunaz S and Quezel G 1967 *Solid State Commun.* **5** 25
Buisson G 1972 *Thesis*, University of Grenoble
—— 1973 *Phys. Status Solidi* **16** 533
Hohlwein D 1975 *Reactor Centrum Nederland Report RCN* 234 pp 410
Knapp B M, Sinclair F and Wilkinson C 1974 *J. Appl. Crystallogr.* **7** 370
Nowik I, Williams H J, Van Uitert L G and Levinstein H J 1966 *J. Appl. Phys.* **37** 970
Schieber M, Grill A, Nowik I, Wanklyn B M Y, Sherwood R C and Van Uitert L G 1973 *J. Appl. Phys.* **44** 1864
Wanklyn B M R 1972 *J. Mater. Sci.* **7** 813
Watson R E and Freeman A J 1961 *Acta Crystallogr.* **14** 27
Wilkinson C 1968 *Phil. Mag.* **17** 609
—— 1973 *Acta Crystallogr.* A**29** 449